Unlocking the synergetic potential of cobalt iron phosphate and multiwalled carbon nanotube composite towards supercapacitor application

Tushar B. Deshmukh[1], Avinash Mendhe[2], Chinmayee Padwal[3], Deepak Dubal[3], Dae-Young Kim[4], Babasaheb R. Sankapal[1*]

[1] Nanomaterial and Device Laboratory, Department of Physics, Visvesvaraya National Institute of Technology, South Ambazari Road, Nagpur, Maharashtra 440010 India.

[2]Department of Electronic Engineering, Kyung Hee University, 1732 Deogyeong-daero, Giheung-gu, Yongin 17104, Republic of Korea

[3]Centre for Materials Science, School of Chemistry and Physics, Queensland University of Technology (QUT), 2 George Street, Brisbane, QLD 4001, Australia

[4]Department of Biological and Environmental Science, College of Life Science and Biotechnology, Dongguk University, 32 Dongguk-ro, Ilsandong-gu, Siksa-dong, 10326 Goyang-si, Gyeonggi-do, South Korea.

Section-I

Characterizations

X-ray diffraction (XRD) patterns for iron phosphate and copper substrate were investigated by Bruker D2-Phaser diffractometer facilities with CuK_α radiation (λ=1.5406 Å), 10 mA applied current, and 30 kV accelerating voltage. The morphological properties of the thin films were captured using a field emission scanning electron microscopy (FESEM, SUPRA – 40 VP, Zeiss Marlin, Germany) and an energy dispersive X-ray spectrometer (EDX). X-ray photoelectron spectroscopy (XPS) was investigated using a Matlab 2000 photoelectron spectrophotometer and consistent AlK X-ray radiations (600 W; hυ = 1486.6 eV). HR-TEM analysis was performed by FEI Tecnai G2F30 (FEI, Netherland).

Electrochemical Study

A potentiostat (Princeton Applied Research, PARSTAT-4000, USA) with a three-electrode configuration, electrochemical capabilities including cyclic voltammetry (CV), galvanostatic charge-discharge (GCD), and electrochemical impedance spectroscopy (EIS) were studied. To investigate all electrochemical characteristics, a working electrode with active area of 1×1 cm^2 was used. A liquid state device was fabricated and electrochemical investigations were carried out through two electrodes configuration.

Section II

Specific capacitance values were calculated by using CV from the following equation[1]

$$C_{sp} = \frac{\int I dV}{m\,v\,(V_f - V_i)} \qquad (S1)$$

Specific capacitance values were calculated by using GCD from the following equation[2].

$$C_{Sp} = \frac{2I\int Vdt}{m(V_f - V_i)^2} \qquad (S2)$$

Where C_{sp} is specific capacitance, i is current density, m is active mass, V_f - V_i potential window or working potential.

Specific Capacity

$$C_s = \frac{\int_{V_1}^{V_2} I(V)dV}{\upsilon m} \qquad (S3)$$

where, Cs is specific capacity (C/g), I (A) is the cathodic or anodic current, dV (V) is the operated potential window, υ (V/s) is the applied scan rate, m (g) is the deposited mass on Cu substrate.

Section-III

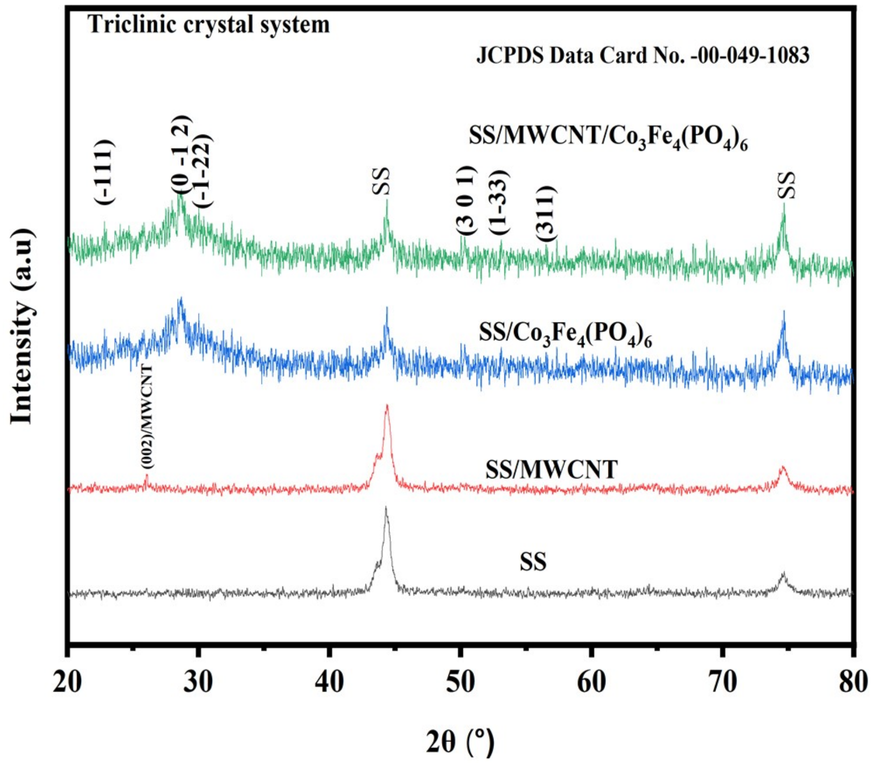

Figure S1: Comparative XRD of SS, MWCNTs, $Co_3Fe_4(PO_4)_6$, and MWCNTs/$Co_3Fe_4(PO_4)_6$.

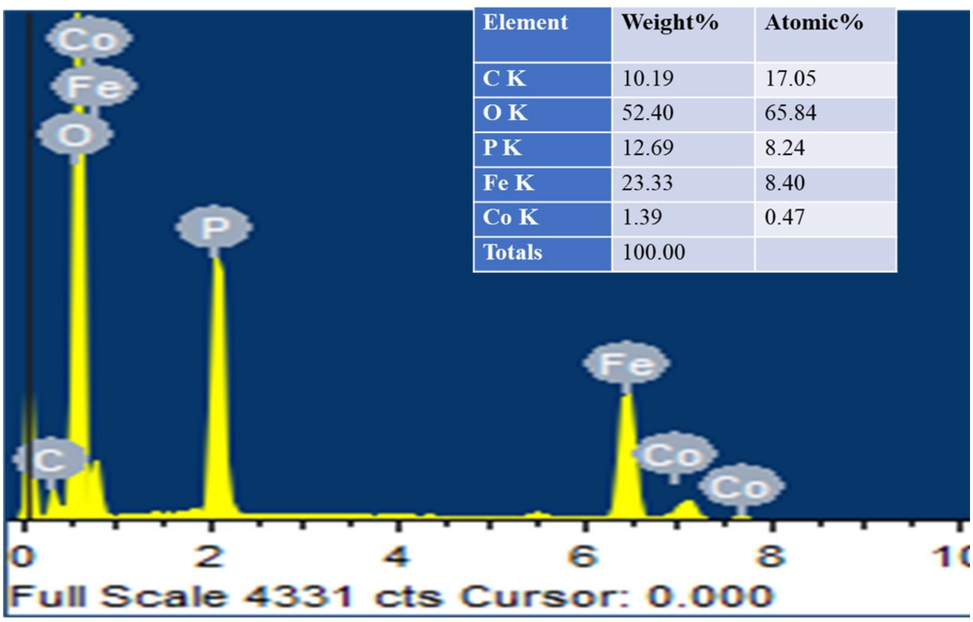

Element	Weight%	Atomic%
C K	10.19	17.05
O K	52.40	65.84
P K	12.69	8.24
Fe K	23.33	8.40
Co K	1.39	0.47
Totals	100.00	

Figure S2 EDX analysis of MWCNTs/$Co_3Fe_4(PO_4)_6$ thin film

In our preceding article, we presented an analysis of the electrochemical performance of $Fe_7(PO_4)_6$[3] and MWCNTs/$Co_2P_2O_7$[4] in a KOH electrolyte. Figure S3 illustrates the comparative cyclic voltammetry (CV) of MWCNTs, $Fe_7(PO_4)_6$, $Co_2P_2O_7$, and MWCNTs/ $CO_3Fe_4(PO_4)_6$. Notably, the potential window of MWCNTs/$Co_3Fe_4(PO_4)_6$ (0.9 V) surpasses that of the previously reported $Fe_7(PO_4)_6$ (0.71 V) and $Co_2P_2O_7$ (0.5 V), indicating a marked enhancement in the electrochemical performance of the bimetallic phosphate. $Co^{+2/+1}$ reduction potential -0.28 V and for $Fe^{+3/+2}$ is 0.77 V, but we didn't observe any sharp reduction peak at -0.28 V and 0.77 V fall out of scanning voltage range. This show the fabricated material is pseudocapacitive material dominated with surface redox activity contributing in the charge

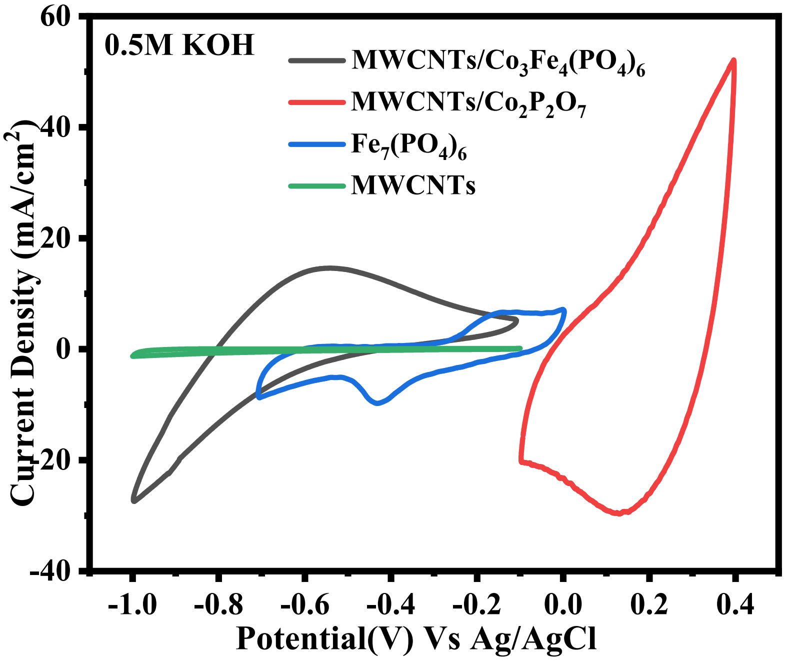

Figure S3 Comparative CV at 100 mV/s of MWCNTs, $Fe_7(PO_4)_6$, $Co_2P_2O_7$, MWCNTs/$Co_3Fe_4(PO_4)_6$.

storage[5–7].

Furthermore, there is a significant improvement in specific capacitances, with MWCNTs/$Co_3Fe_4(PO_4)_6$ exhibiting a specific capacitance of 859 C/g, compared to 450 C/g for $Co_2P_2O_7$ and 104 C/g (147 F/g) for $Fe_7(PO_4)_6$. This improvement underscores the enhanced efficacy of the bimetallic phosphate in energy storage due to synergetic effect between $CO_3Fe_4(PO_4)_6$ and MWCNTs. In Figure S3, the area under the curve for MWCNT/$Co_2P_2O_7$ is indeed large, mainly due to its higher mass loading of 1.7 mg compared to MWCNT/Co3Fe4(PO4)6 with only 0.2 mg. This higher mass loading contributes to its lower specific capacitance. Additionally, the potential window of the electrode is also higher by 0.4 V for MWCNT/$Co_3Fe_4(PO_4)_6$ compared to MWCNT/$Co_2P_2O_7$, indicating the superiority of MWCNT/$Co_3Fe_4(PO_4)_6$.

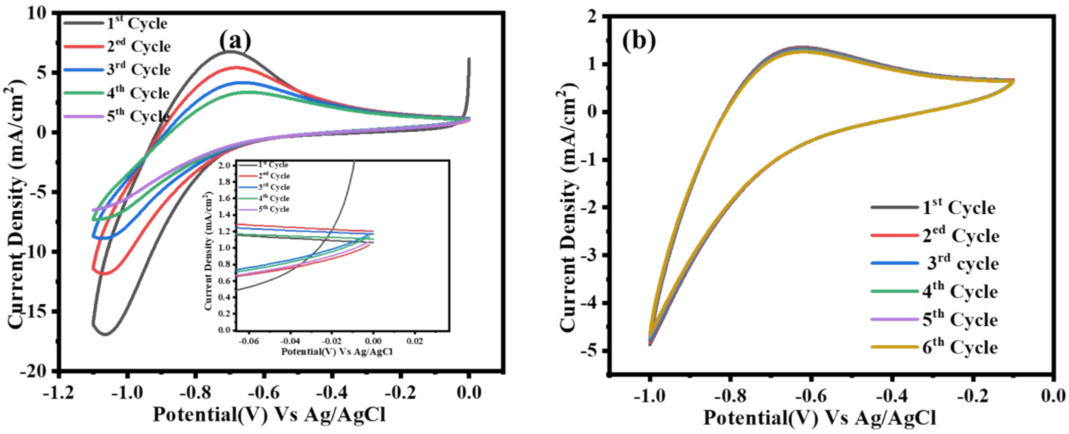

Figure S4 (a) CV analysis in potential range 0 to -1.1 V (b) CV analysis in potential range -0.1 to -1 V

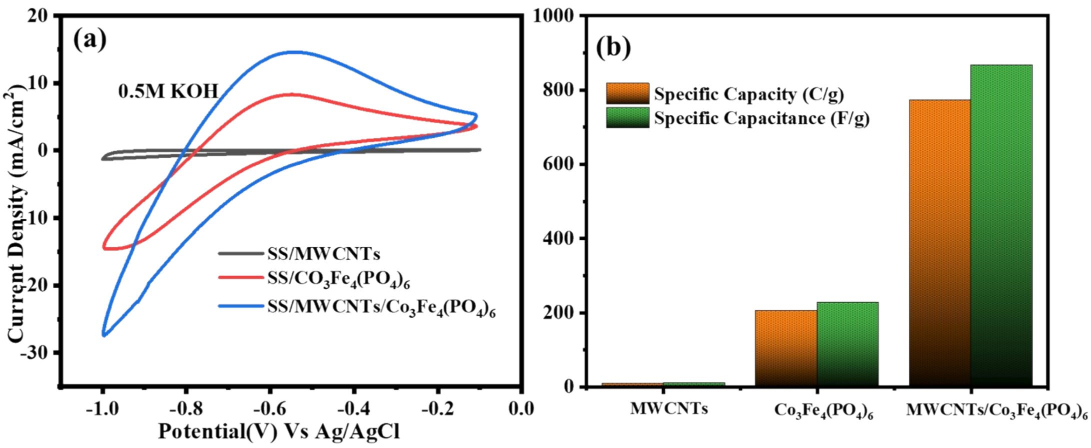

Figure S5 (a) CV of $Co_3Fe_4(PO_4)_6$, MWCNTs, and MWCNTs/$Co_3Fe_4(PO_4)_6$ in 0.5 M KOH (b) corresponding Specific capacity and specific capacitance with different electrode

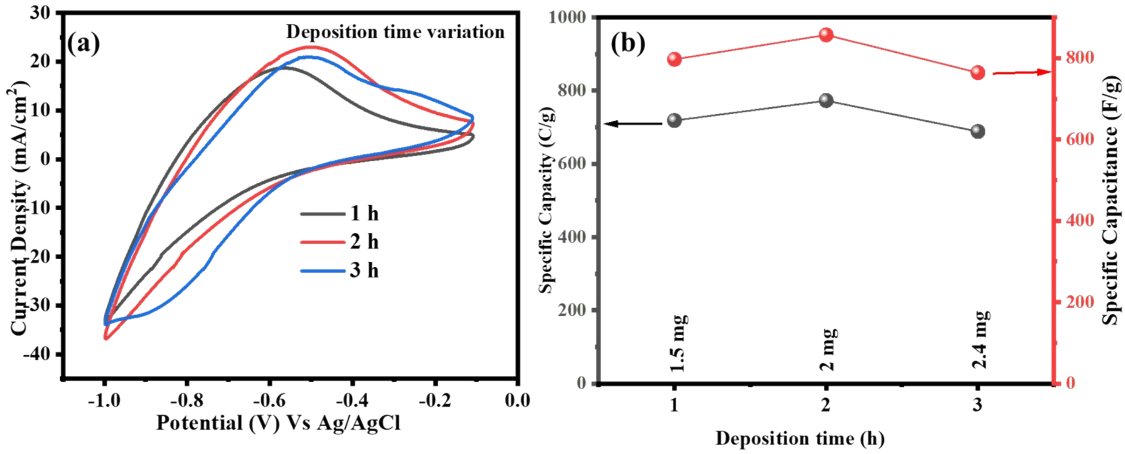

Figure S6 (a) CV of $Co_3Fe_4(PO_4)_6$, MWCNTs, and MWCNTs/$Co_3Fe_4(PO_4)_6$ in 0.5 M KOH (b) specific capacity and capacitance of deposition time varied electrode

1

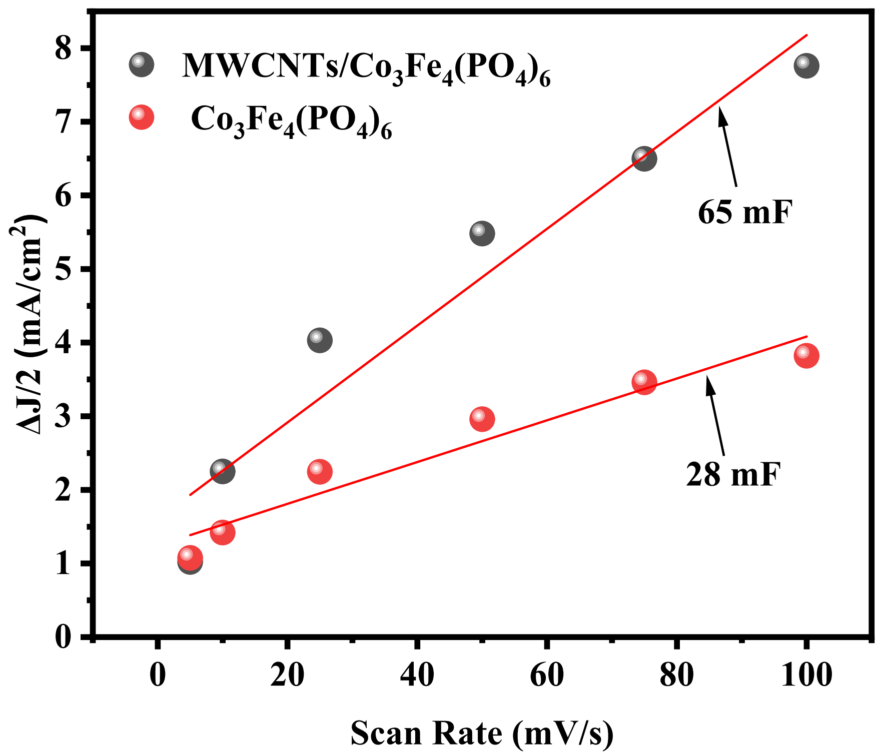

Figure S7 $\Delta j/2$ vs. scan rate

1

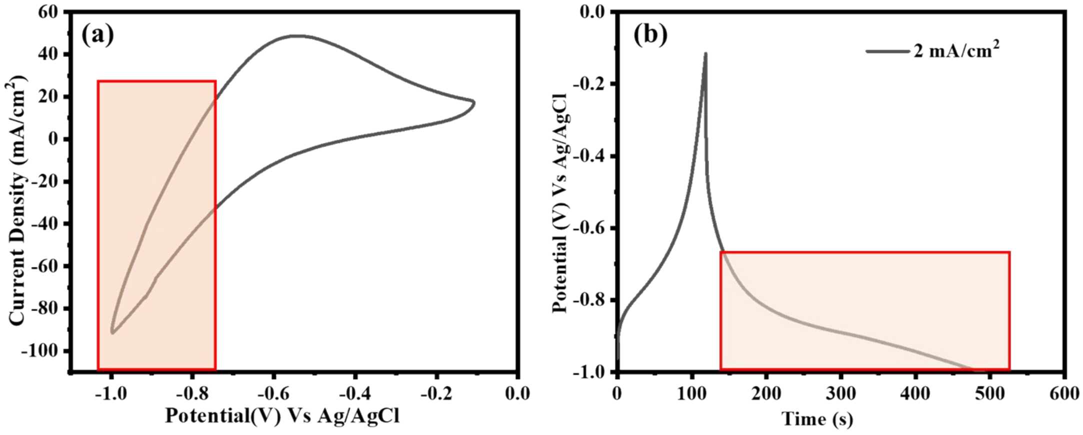

Figure S8 (a) CV at 100 mV/s scan rate (b) GCD at 2 mA/cm^2

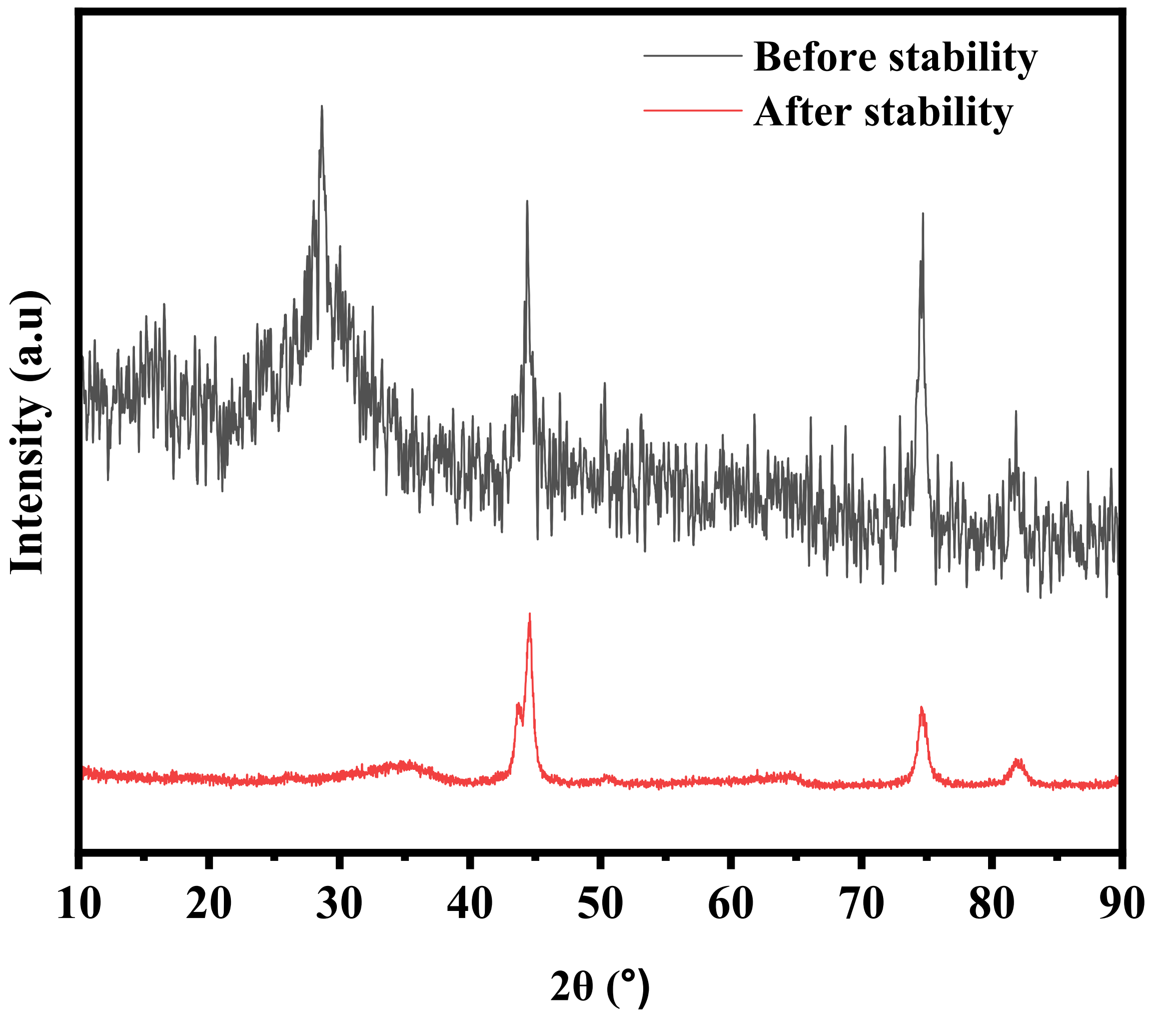

Figure S9 XRD investigation before and after complete electrochemical investigation

1

Table No S1 XPS peak assignment		
Sr. No	**Binding energy (eV)**	**Assigned peak**
1	29.1	P3s
2	58.2	Fe3p
3	135	P2p
4	194.1	P2s
5	285.1	C1s
6	533.1	O1s
7	712 to 735	Fe2p
8	779 to 800	Co2p
9	979	OKL1
10	999	OKL2

Table No S2 EIS Fittings valves	
Component	**Value**
R_s (Ω/cm^2)	3.852
C_{dl1} (F/cm^2)	0.000309
R_{ct} (Ω/cm^2)	0.9664
C_{dl2} (F/cm^2)	0.001625
R_L (Ω/cm^2)	0.5411
W	0.1484

References

1 B. Pandit, D. P. Dubal and B. R. Sankapal, *Electrochim. Acta*, 2017, **242**, 382–389.

2 H. M. El Sharkawy, D. M. Sayed, A. S. Dhmees, R. M. Aboushahba and N. K. Allam, *ACS Appl. Energy Mater.*, 2020, **3**, 9305–9314.

3 T. B. Deshmukh, P. Babar, T. Kedara Shivasharma and B. R. Sankapal, *Surfaces and Interfaces*, 2022, **35**, 102419.

4 A. Agarwal and B. R. Sankapal, *Sustain. Energy Fuels*, 2022, **6**, 4085–4101.

5 F. Scholz, *Electroanalytical methods: Guide to experiments and applications*, 2010.

6 S. Azmi and E. Frackowiak, *Electrochem. commun.*, 2022, **138**, 107289.

7 S. Shiraishi, *Electric Double Layer Capacitor*, Elsevier Ltd, 2016, vol. 2.